Automatica 130 (2021) 109690

Contents lists available at ScienceDirect

Automatica

journal homepage: www.elsevier.com/locate/automatica

Brief paper

Boundary adaptive fault-tolerant control for a flexible Timoshenko arm with backlash-like hysteresis☆

Zhijia Zhao [a], Zhijie Liu [b,*], Wei He [b], Keum-Shik Hong [c], Han-Xiong Li [d]

[a] School of Mechanical and Electrical Engineering, Guangzhou University, Guangzhou 510006, China
[b] School of Automation and Electrical Engineering, University of Science and Technology Beijing, Beijing 100083, China
[c] School of Mechanical Engineering, Pusan National University, 2 Busandaehak-ro, Guemjeong-gu, Busan 46241, Republic of Korea
[d] Department of Systems Engineering and Engineering Management, City University of Hong Kong, Hong Kong

ARTICLE INFO

Article history:
Received 6 May 2020
Received in revised form 9 February 2021
Accepted 31 March 2021
Available online 13 May 2021

Keywords:
Timoshenko arm
Adaptive fault-tolerant control
Actuator failure
Backlash-like hysteresis
Vibration control

ABSTRACT

This study is concerned with a novel adaptive fault-tolerant control design for a flexible Timoshenko arm considering the effects of actuator failures, backlash-like hysteresis, and external disturbances. First, the actuator failures and backlash-like hysteresis are integrated together and resolved into desired control signals and nonlinear errors. Second, these errors and external disturbances are deemed as composite disturbance terms to be handled with adaptive techniques. Third, adaptive fault-tolerant controllers with online updates are established to eliminate the shear deformation and elastic oscillation, lay the arm in a desired angle, counteract the hybrid effects of actuator failures and hysteresis, and deal with the uncertainty of composite disturbances. Then, based on the Lyapunov's stability theory, the proposed strategy guarantees the uniformly bounded stability in the controlled system. Finally, numerical examples are presented to illustrate the efficacy of the suggested scheme.

1. Introduction

Manipulators are extensively applied in aerospace, navigation, agriculture, construction, manufacturing, healthcare and other fields (Guo, Pan, Zheng, & Yu, 2020; He, Gao, Zhou, Yang, & Li, 2020). Flexible manipulators have a wide range of applications than rigid ones depending on their advantages of lower energy consumption, light weight, high efficiency, large operating space, and high-speed operation (Goubej, Vyhlídal, & Schlegel, 2020; Zhao, He, & Ahn, 2019). In harsh environments and working conditions, vibration and deformation frequently appear in flexible manipulators, which would produce adverse effects such as system performance deterioration and limited production accuracy. Consequently, there is an urgent need to establish efficient control methodologies for dampening vibrations in flexible manipulators.

Over the past 10 years, many researchers have dedicated themselves to seeking various control techniques, such as mode order reduction method (MORM) (He et al., 2020) and boundary control (Zhao et al., 2019) to restrain vibrations and improve performances in flexible manipulator systems. A finite-dimensional system represented by ordinary differential equations (ODEs) is extracted from an infinite-dimensional system described by partial differential equations (PDEs) with the help of the MORM method, and spillover instabilities from model truncation will arise. Boundary control can circumvent the above problem and is nonintrusively sensed and actuated, thus it is considered to be an efficient and practical solution. Great strides have been witnessed in boundary control of flexible manipulators in recent years (Zhao et al., 2019). To simplify the system analysis, the research mentioned above concentrated on the elastic oscillation and angle position without considering the shear deformation in the flexible link. Provided that the nonlinear coupling of angle position, shear deformation, and elastic deflection is incorporated into the system dynamics, significant challenges may be posed to the design and analysis. Recently, boundary control for flexible Timoshenko manipulators has been significantly developed in Endo, Sasaki, Matsuno, and Jia (2017), He, He, and Sun (2017) and Zhao and Ahn (2020). The literature of Endo et al. (2017) resolved contact-force control issues and explored the exponential stabilization of controlled systems. In Zhao and Ahn (2020), vibration suppression and saturation elimination in Timoshenko manipulators were realized via an antisaturation scheme. The authors in He et al. (2017) addressed the vibration attenuation and constraint handling in uncertain Timoshenko manipulators by constructing an adaptive barrier-based control.

☆ The material in this paper was not presented at any conference. This paper was recommended for publication in revised form by Associate Editor Angelo Alessandri under the direction of Editor Thomas Parisini.

* Corresponding author.
E-mail addresses: zhjzhaoscut@163.com (Z. Zhao), liuzhijie2012@gmail.com (Z. Liu), hewei.ac@gmail.com (W. He), kshong@pusan.ac.k (K.-S. Hong), mehxli@cityu.edu.hk (H.-X. Li).

https://doi.org/10.1016/j.automatica.2021.109690
0005-1098/

Hysteresis is a dynamic nonsmooth nonlinearity and generally found in electronic, magnetic, electromagnetic, biophotoelectric, and other types of system components (Zhang, Liu, Dai, & Wang, 2020). Nonsmooth hysteresis nonlinearity becomes the key limited factor in dynamic performance of control systems due to itself non-differentiability. Neglecting the hysteresis nonlinearity can result in unpredictable inaccuracies or oscillations and even instability. To efficiently handle the hysteresis, several researchers have focused on developing diverse control techniques in recent years (Ibrir & Su, 2017; Su, Stepanenko, Svoboda, & Leung, 2000; Yu, Li, Yu, & Li, 2018). In Yu et al. (2018), an observer-based adaptive neural control was constructed to stabilize stochastic nonlinear systems considering the effects of unknown control directions and backlash-like hysteresis. The authors in Ibrir and Su (2017) and Su et al. (2000) discussed the adaptive robust control for nonlinear systems influenced by several kinds of hysteresis inputs. However, note that the aforesaid research results were limited to control design of finite-dimensional ODE systems with hysteresis and these approaches cannot be directly applied to infinite-dimensional PDE systems.

Actuator faults inevitably occur in various industrial control processes due to widespread uncertainties and external complex interferences (Boem, Riverso, Ferrari-Trecate, & Parisini, 2019; Khalili, Zhang, Polycarpou, Parisini, & Cao, 2018; Liu, Han, Zhao, & He, 2020; Yang et al., 2020). The existence of faults generally gives rise to adverse reactions and shut-down of controlled systems results in technical component damages, and even leads to production accidents (Dong, Tao, Wen, & Jiang, 2019; Khalili, Zhang, Cao, Polycarpou, & Parisini, 2020; Wang, Liu, Zhao, & Liu, 2020). Consequently, fault-tolerant control (FTC) has become one of key control objectives in the course of control design for safety purpose. For the past few years, fruitful research achievements on FTC have been achieved for engineering control PDE systems. In Cao and Liu (2019), adaptive FTC strategies were put forward to ensure the vibration damping control and eliminate actuator failures in 3D manipulator systems. However, the FTC design presented in Cao and Liu (2019) was only available for flexible Euler manipulator systems, and the method cannot be directly applied to flexible Timoshenko manipulators with shear deformation. Moreover, the literature (Cao & Liu, 2019) was confined to eliminating the oscillation and compensating actuator failures, and the hybrid effects of actuator failures, hysteresis nonlinearity, and external disturbances was not taken into account during the design. To the best of our knowledge, although advances in the study of FTC for flexible manipulators have been significantly achieved, no research has been reported thus far on developing an adaptive FTC control for stabilizing flexible Timoshenko manipulators with actuator failures, hysteresis nonlinearity, and external disturbances, which motivates this research.

Different from the existing results on adaptive control of 1-dimensional PDEs without coupling (Koga & Krstic, 2020; Wang & Krstic, 2020), in this paper, we are going to establish an adaptive FTC for stabilizing and controlling a coupled flexible Timoshenko arm influenced by actuator failures, backlash-like hysteresis, and external disturbances. The main contributions are listed as follows: (i) By incorporating actuator failures and backlash-like hysteresis and disintegrating the resulting equations into desired control signals and nonlinear errors, composite disturbance terms are generated from errors and external disturbances. (ii) Three novel adaptive fault-tolerant controllers with unknown upper-bound updated online are developed to suppress the shear deformation and elastic oscillation, achieve the joint angle control, and compensate for the hybrid effects of actuator failures, backlash-like hysteresis, and uncertainties of composite disturbances. (iii) The established control schemes can achieve the boundary-controlled system's uniformly bounded stability without simplifying or discretizing infinite-dimensional system dynamics.

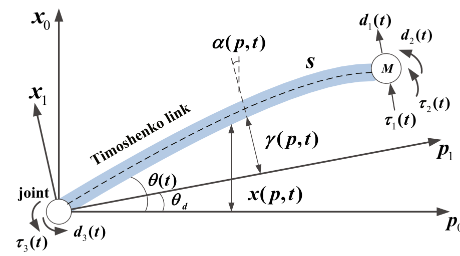

Fig. 1. A flexible Timoshenko arm.

2. Problem statement

A vibrating flexible Timoshenko arm system is illustrated in Fig. 1. Let t and p be independent time and spatial variables. $\gamma(p,t)$ describes the elastic deflection of the arm with length s, inertia per unit length I_ρ, mass of unit length ρ, cross-sectional area B, and bending stiffness EI. $\alpha(p,t)$, $\theta(t)$, and θ_d represent the rotation of the arm's cross-section, the hub's angle position, and a desired angle position, respectively, with an angle error defined as $e(t) = \theta(t) - \theta_d$. The displacement $x(p,t)$ is formulated as $x(p,t) = p\theta(t) + \gamma(p,t)$. $\tau_3(t)$ denotes the control input torque on the hub with inertia I_h. $\tau_1(t)$ and $\tau_2(t)$ represent the control input and control torque acting on the tip payload with inertia J and mass M, respectively. $d_i(t), i = 1, 2, 3$ are external disturbances. We define notations as $(\star)' = \partial(\star)/\partial p$, $\dot{(\star)} = \partial(\star)/\partial t$, $(\star)'' = \partial^2(\star)/\partial p^2$, and $\ddot{(\star)} = \partial^2(\star)/\partial t^2$.

2.1. System model

The dynamics of the Timoshenko arm system under consideration in this study is given directly as (He, He, Qin, & Sun, 2018)

$$\rho\ddot{x} + K\alpha' - K\gamma'' = 0, 0 < p < s, \tag{1}$$

$$I_\rho\ddot{\alpha} - K(\gamma' - \alpha) - EI\alpha'' = 0, 0 < p < s, \tag{2}$$

$$\alpha(0,t) = \gamma(0,t) = 0, \tag{3}$$

$$M\ddot{x}(s,t) - K\alpha(s,t) + K\gamma'(s,t) - d_1(t) - \tau_1(t) = 0, \tag{4}$$

$$J\ddot{\alpha}(s,t) + EI\alpha'(s,t) - d_2(t) - \tau_2(t) = 0, \tag{5}$$

$$I_h\ddot{\theta}(t) + K[\int_0^s \alpha dp - \gamma(s,t)] - d_3(t) - \tau_3(t) = 0, \tag{6}$$

where $K = cBR$, R represents the shear modulus, and c denotes a positive constant concerning the cross-sectional shape.

Remark 1. Unlike the existing results (Endo et al., 2017; Morgul, 1991; Shi, Feng, , & Yan, 2001), in this paper, the modeling of the Timoshenko arm is relatively complex and difficult given the coupling of the elastic deformation, shear deformation, angle position, and load dynamics, which is mainly based on the rotational Timoshenko beam/arm theory. However, considering the different actual situation, the system model may be slightly different from the previous works (Endo et al., 2017; Morgul, 1991; Shi et al., 2001). In addition, the proposed approaches validate the system model through subsequent analysis, proof, and simulation.

2.2. Actuator Fault and Backlash-Like Hysteresis

In this study, we consider an actuator subject to partial failures described by

$$\tau_i(t) = \varsigma_i v_i(t), \tag{7}$$

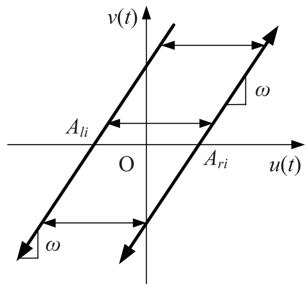

Fig. 2. Backlash nonlinearity.

where $0 < \varsigma_i \leq 1, i = 1, 2, 3$ denote the failure extent of actuators and $v_i(t), i = 1, 2, 3$ describe ideal control inputs with no failures.

As shown in Fig. 2, the analytical expression of the backlash nonlinearity (Tao & Kokotovic, 1996; Zhou, Zhang, & Wen, 2007) is given as

$$\dot{v}_i(t) = \begin{cases} \omega\dot{u}_i(t), & \text{if } \dot{u}_i > 0 \text{ and } v_i(t) = \omega(u_i(t) - A_{ri}), \\ & \text{or if } \dot{u}_i < 0 \text{ and } v_i(t) = \omega(u_i(t) - A_{li}) \\ 0, & \text{otherwise,} \end{cases} \tag{8}$$

where $\omega > 0$ represents the slope, A_{ri} and A_{li} denote constant scalars, $u_i(t)$ denotes the control laws to be designed in the following, i.e., the backlash-like hysteresis input, and the motion on any inner segment is characterized by $\dot{u}_i(t) = 0$.

According to (8), we consider the flexible Timoshenko arm system subject to backlash-like hysteresis operator $v_i(u_i(t)), i = 1, 2, 3$ defined by

$$v_i(u_i(t)) = \begin{cases} \omega(u_i(t) - A_{ri}), & \text{if } \dot{u}_i > 0 \text{ and } v_i(t) = \omega(u_i(t) - A_{ri}) \\ \omega(u_i(t) - A_{li}), & \text{if } \dot{u}_i < 0 \text{ and } v_i(t) = \omega(u_i(t) - A_{li}) \\ v_i(u_i(t\_)), & \text{otherwise,} \end{cases} \tag{9}$$

where $v_i(u_i(t\_))$ signifies that the backlash-like hysteresis output $v_i(u_i(t))$ keeps its previous value when $\dot{u}_i(t) = 0$.

Invoking Tao and Kokotovic (1996) and Zhou et al. (2007), we can formulate the hysteresis $v_i(u_i(t))$ as

$$\begin{aligned} v_i(u_i(t)) =& \eta_{ri}(t)\omega(u_i(t) - A_{ri}) + \eta_{li}(t)\omega(u_i(t) - A_{li}) \\ &+ \eta_{si}(t)u_{si}, \end{aligned} \tag{10}$$

where

$$\eta_{ri}(t) = \begin{cases} 1, & \text{if } \dot{v}_i > 0 \\ 0, & \text{otherwise} \end{cases} \tag{11}$$

$$\eta_{li}(t) = \begin{cases} 1, & \text{if } \dot{v}_i < 0 \\ 0, & \text{otherwise} \end{cases} \tag{12}$$

$$\eta_{si}(t) = \begin{cases} 1, & \text{if } \dot{v}_i = 0 \\ 0, & \text{otherwise.} \end{cases} \tag{13}$$

The generic constant u_{si} in (10) satisfies the following inequality constraint:

$$\omega(u_i(t) - A_{ri}) \leq u_{si} \leq \omega(u_i(t) - A_{li}). \tag{14}$$

It can be obtained from (11)–(13) that $\eta_{ri}(t)+\eta_{li}(t)+\eta_{si}(t) = 1$ holds for all t. Combining (10) and (14), we can rewritten the hysteresis $v_i(u_i(t))$ as

$$v_i(u_i(t)) = \omega u_i(t) + \sigma(u_i(t)), \tag{15}$$

where $\sigma(u_i(t))$ is denoted as

$$\sigma(u_i(t)) = \begin{cases} -\omega A_{ri}, & \text{if } \dot{u}_i > 0 \\ -\omega A_{li}, & \text{if } \dot{u}_i < 0 \\ \zeta(u_i(t)), & \text{if } \dot{u}_i = 0, -\omega A_{ri} \leq \zeta(u_i(t)) \leq -\omega A_{li}. \end{cases} \tag{16}$$

Remark 2. As stated in Su et al. (2000), $\sigma(u_i(t))$ has an explicit solution and is bounded. It is evident that the bound of $\sigma(u_i(t))$ depends on A_{li}, A_{ri}, and ω.

Invoking (7) and (15) gives

$$\tau_i(t) = \varsigma_i\omega u_i(t) + \varsigma_i\sigma(u_i(t)). \tag{17}$$

Applying (17) on (4)–(6) yields

$$\begin{aligned} M\ddot{x}(s,t) - K\alpha(s,t) + K\gamma'(s,t) - d_1(t) - \varsigma_1\omega u_1(t) \\ - \varsigma_1\sigma(u_1(t)) = 0, \end{aligned} \tag{18}$$

$$\begin{aligned} J\ddot{\alpha}(s,t) + EI\alpha'(s,t) - d_2(t) - \varsigma_2\omega u_2(t) \\ - \varsigma_2\sigma(u_2(t)) = 0, \end{aligned} \tag{19}$$

$$\begin{aligned} I_h\ddot{\theta}(t) + K[\int_0^s \alpha dp - \gamma(s,t)] - d_3(t) - \varsigma_3\omega u_3(t) \\ - \varsigma_3\sigma(u_3(t)) = 0. \end{aligned} \tag{20}$$

2.3. Preliminaries

We first put forward the following lemmas and assumption:

Lemma 1 (*Zhao et al., 2019*)**.** *Let $\nu(p,t), \nu_1(p,t), \nu_2(p,t) \in \mathbb{R}$ with $(p,t) \in [0,s] \times [0,+\infty)$. The following inequalities are derived for $\psi > 0$ and $\nu(0,t) = 0$:*

$$\nu_1(p,t)\nu_2(p,t) \leq \psi\nu_2^2(p,t) + \frac{1}{\psi}\nu_1^2(p,t), \tag{21}$$

$$\nu^2 \leq s\int_0^s \nu'^2 dp, \int_0^s \nu^2 dp \leq s^2\int_0^s \nu'^2 dp. \tag{22}$$

Lemma 2 (*Polycarpou & Ioannou, 1996*)**.** *For any $\nu(s,t) \in \mathbb{R}$, we have the following inequality:*

$$0 \leq |\nu(s,t)| - \nu(s,t)\tanh(\nu(s,t)) \leq a. \tag{23}$$

where $a = 0.2785$.

Assumption 1. For $d_j(t), j = 1\cdots 3$, we suppose that there exist $\varrho_j > 0, j = 1\cdots 3$ such that $|\ d_1(t)\ | \leq \varrho_1$, $|\ d_2(t)\ | \leq \varrho_2$, and $|\ d_3(t)\ | \leq \varrho_3$, $\forall t \in [0,+\infty)$.

3. Control design

In this section, the extraneous disturbances and hysteresis error are first identified as composite disturbances. Subsequently, the adaptive FTCs and dynamically updating laws are developed to stabilize the shear deformation and elastic oscillation, realize the angle control, and eliminate the hybrid effects of actuator failures, hysteresis, and unknown upper-bound of composite disturbances. The control block diagram is depicted in Fig. 3.

3.1. Boundary control

First, we define

$$Q_i(t) = d_i(t) + \varsigma_i\sigma(u_i(t)). \tag{24}$$

Invoking (24), (18)–(20) can be rewritten as

$$M\ddot{x}(s,t) - K\alpha(s,t) + K\gamma'(s,t) - Q_1(t) - \varsigma_1\omega u_1(t) = 0, \tag{25}$$

$$J\ddot{\alpha}(s,t) + EI\alpha'(s,t) - Q_2(t) - \varsigma_2\omega u_2(t) = 0, \tag{26}$$

$$I_h\ddot{\theta}(t) + K[\int_0^s \alpha dp - \gamma(s,t)] - Q_3(t) - \varsigma_3\omega u_3(t) = 0. \tag{27}$$

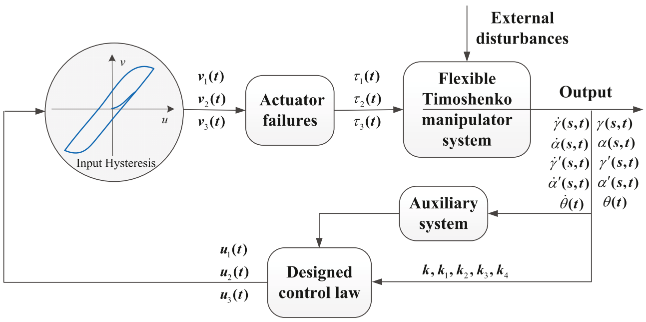

Fig. 3. Control block diagram.

Considering $0 < \varsigma_i \leq 1, i = 1, 2, 3$, (16), Assumption 1, and Remark 1, we can derive that there exist positive constants $Q_{im}, i = 1, 2, 3$ satisfying $|Q_i(t)| \leq Q_{im}, i = 1, 2, 3$. Then, $Q_i(t), i = 1, 2, 3$ can be regarded as composite disturbance terms to be handled with adaptive techniques. Let $\tilde{Q}_{im}(t)$ be the estimate values of $\hat{Q}_{im}(t)$ and the estimate errors are defined as $\tilde{Q}_{im} = \hat{Q}_{im} - Q_{im}, i = 1, 2, 3$.

For ease of design, let $q_i = \frac{1}{\varsigma_i}, i = 1, 2, 3$, $\hat{q}_i, i = 1, 2, 3$ represent the estimate values of failure parameters and estimation errors are defined as $\tilde{q}_i = \hat{q}_i - q_i$. Then, we construct the auxiliary signals $\varpi_1(t)$, $\varpi_2(t)$, and $\varpi_3(t)$ as

$$\varpi_1(t) = \dot{x}(s, t) - \alpha(s, t) + \gamma'(s, t), \tag{28}$$

$$\varpi_2(t) = \dot{\alpha}(s, t) + \alpha'(s, t), \;\; \varpi_3(t) = e(t) + \dot{\theta}(t). \tag{29}$$

Now, the following boundary adaptive fault-tolerant controllers are presented as

$$u_1(t) = \hat{q}_1 f_1(t), \;\; u_2(t) = \hat{q}_2 f_2(t), \;\; u_3(t) = \hat{q}_3 f_3(t), \tag{30}$$

where the auxiliary functions $f_1(t)$, $f_2(t)$, and $f_3(t)$ and adaptive updating laws are designed as

$$\begin{aligned} f_1(t) =& \frac{1}{\omega}\{-K[\alpha(s, t) - \gamma'(s, t)] + M[\dot{\alpha}(s, t) - \dot{\gamma}'(s, t)] \\ & - k\varpi_1(t) - \tanh(\varpi_1(t))\hat{Q}_{1m}\}, \end{aligned} \tag{31}$$

$$\begin{aligned} f_2(t) =& \frac{1}{\omega}\{-k_1\varpi_2(t) + EI\alpha'(s, t) - J\dot{\alpha}'(s, t) \\ & - \tanh(\varpi_2(t))\hat{Q}_{2m}\}, \end{aligned} \tag{32}$$

$$\begin{aligned} f_3(t) =& \frac{1}{\omega}\{-k_2\varpi_3(t) - k_3 e(t) - I_h\dot{\theta}(t) \\ & - k_4\dot{\theta}(t) - \tanh(\varpi_3(t))\hat{Q}_{3m}\}, \end{aligned} \tag{33}$$

$$\dot{\hat{q}}_i = -\varpi_i \omega f_i - \phi_i \hat{q}_i, i = 1, 2, 3, \tag{34}$$

$$\dot{\hat{Q}}_{im} = \varpi_i \tanh(\varpi_i) - \varphi_i \hat{Q}_{im}, i = 1, 2, 3, \tag{35}$$

in which $k, k_1, k_2, k_3, k_4 > 0$ and $\phi_i, \varphi_i > 0, i = 1, 2, 3$ denote the modification terms.

Remark 3. The signals in the proposed control laws (30)–(33) are obtainable during execution. Laser displacement sensors can be employed to measure $\gamma(s, t)$, and inclinometers can be used to measure $\theta(t)$, $\gamma'(s, t)$, and $\alpha(s, t)$. Moreover, we can exploit backward difference algorithms to acquire the signals $\dot{\gamma}'(s, t)$, $\dot{\gamma}(s, t)$, $\dot{\alpha}(s, t)$, $\dot{\alpha}'(s, t)$, and $\dot{\theta}(t)$ with the help of the measured values. $u_1(t)$ can be implemented by designing actuators acting on a cart which connects to the tip payload (Canbolat, Dawson, Rahn, & Nagarkatti, 1998), piezoelectric material (ionic polymer metal composites) (Bandopadhya, Bhattacharya, & Dutta, 2007), the jet actuator and so on. $u_2(t)$ can be realized by mounting a motor or a piezoelectric material at the free-end of the tip payload. $u_3(t)$ can be achieved by a servo motor to make this link track a desired angle position.

Remark 4. Different from the backlash-inverse handling approaches mentioned in Giri, Radouane, Brouri, and Chaoui (2014) and Giri, Rochdi, Radouane, Brouri, and Chaoui (2013), in this paper, we first integrate the backlash-like hysteresis with actuator failures and resolve it into desired control signals and nonlinear errors. Subsequently, adaptive techniques are adopted to handle composite disturbance terms composed with nonlinear errors and external disturbances.

Set a Lyapunov candidate function as

$$G(t) = G_m(t) + G_n(t) + G_p(t) + G_o(t), \tag{36}$$

where

$$\begin{aligned} G_m(t) =& \frac{1}{2}\rho \int_0^s \dot{x}^2 dp + \frac{1}{2} I_\rho \int_0^s \dot{\alpha}^2 dp \\ & + \frac{1}{2} EI \int_0^s \alpha'^2 dp + \frac{1}{2} K \int_0^s (\gamma' - \alpha)^2 dp, \end{aligned} \tag{37}$$

$$\begin{aligned} G_n(t) =& \frac{1}{2} M\varpi_1^2(t) + \frac{1}{2} J\varpi_2^2(t) + \frac{1}{2} I_h \varpi_3^2(t) \\ & + \frac{1}{2}(k_3 + k_4)e^2(t), \end{aligned} \tag{38}$$

$$\begin{aligned} G_p(t) =& \epsilon\rho \int_0^s p\gamma'\dot{x} dp + \epsilon I_\rho \int_0^s p\alpha'\dot{\alpha} dp \\ & + \kappa\epsilon I_\rho \int_0^s \alpha\dot{\alpha} dp, \end{aligned} \tag{39}$$

$$G_o(t) = \frac{\varsigma_i}{2}\tilde{q}_i^2 + \frac{1}{2}\tilde{Q}_{im}^2, i = 1, 2, 3 \tag{40}$$

with $\epsilon, \kappa > 0$.

Lemma 3. *The selected function in (36) is a positive definite function as*

$$\begin{aligned} 0 \leq& \delta_1[G_m(t) + G_n(t) + G_o(t)] \leq G(t) \\ & \leq \delta_2[G_m(t) + G_n(t) + G_o(t)], \end{aligned} \tag{41}$$

where $\delta_1, \delta_2 > 0$.

Proof. Applying Lemmas 1 to (39) generates

$$\begin{aligned} |G_p(t)| \leq& [\epsilon I_\rho s + (\kappa\epsilon I_\rho + 14\epsilon\rho s)s^2] \int_0^s \alpha'^2 dp \\ & + 2\epsilon\rho s \int_0^s (\gamma' - \alpha)^2 dp + \epsilon\rho s \int_0^s \dot{x}^2 dp \\ & + (\epsilon I_\rho s + \kappa\epsilon I_\rho) \int_0^s \dot{\alpha}^2 dp \leq \iota G_m(t), \end{aligned} \tag{42}$$

where $\iota = \frac{2\epsilon \max\left(2\rho s, (s+\kappa)I_\rho, [I_\rho s + (\kappa I_\rho + 14\rho)s^2]\right)}{\min(\rho, I_\rho, EI, K)}$.

From the above equation, we have

$$-\iota G_m(t) \leq G_p(t) \leq \iota G_m(t). \tag{43}$$

We properly choose parameters ϵ and κ to yield

$$0 \leq \iota_1 G_m(t) \leq G_m(t) + G_p(t) \leq \iota_2 G_m(t), \tag{44}$$

where $\iota_1 = 1 - \iota > 0, \iota_2 = 1 + \iota > 0$. Then, we further obtain

$$\begin{aligned} 0 \leq& \delta_1[G_m(t) + G_n(t) + G_o(t)] \leq G(t) \\ & \leq \delta_2[G_m(t) + G_n(t) + G_o(t)], \end{aligned} \tag{45}$$

where $\delta_1 = \min(1, \iota_1) > 0, \delta_2 = \max(1, \iota_2) > 0$. ■

Lemma 4. *The derivative of (36) is upper bounded as*

$$\dot{G}(t) \leq -\delta G(t) + \sigma, \tag{46}$$

where $\delta, \sigma > 0$.

Proof. The differentiation of (36) is presented as

$$\dot{G}(t) = \dot{G}_m(t) + \dot{G}_n(t) + \dot{G}_p(t) + \dot{G}_o(t). \tag{47}$$

Employing (1) and (2), $\dot{G_m}(t)$ is deduced as

$$\begin{aligned}\dot{G}_m(t) =& K\int_0^s \dot{\theta}(t)\alpha dp - K\dot{\theta}(t)\gamma(s,t) - \frac{K}{2}\dot{x}^2(s,t) \\ &- \frac{K}{2}[\alpha(s,t) - \gamma'(s,t)]^2 - \frac{EI}{2}\alpha'^2(s,t) \\ &- \frac{EI}{2}\dot{\alpha}^2(s,t) + \frac{EI}{2}\varpi_2^2(t) + \frac{K}{2}\varpi_1^2(t).\end{aligned} \tag{48}$$

Differentiating (38) and substituting (4)–(6) and AFT controllers (30), we arrive at

$$\begin{aligned}\dot{G}_n(t) =& \varpi_1(t)[K[\alpha(s,t) - \gamma'(s,t)] + Q_1(t) + \varsigma_1\omega\hat{q}_1 f_1(t) \\ &- M(\dot{\alpha}(s,t) - \dot{\gamma}'(s,t))] + \varpi_2(t)[Q_2(t) \\ &+ \varsigma_2\omega\hat{q}_2 f_2(t) - EI\alpha'(s,t) + J\dot{\alpha}'(s,t)] \\ &+ \varpi_3(t)[I_h\dot{e}(t) - K[\int_0^s \alpha dp - \gamma(s,t)] + Q_3(t) \\ &+ \varsigma_3\omega\hat{q}_3 f_3(t)] + (k_3 + k_4)e(t)\dot{e}(t).\end{aligned} \tag{49}$$

Using Lemmas 1, $\dot{G}_p(t)$ is inferred as

$$\begin{aligned}\dot{G}_p(t) \leq& -\frac{\epsilon EI}{2}\int_0^s \alpha'^2 dp + \frac{\epsilon\rho s}{2}\dot{x}^2(s,t) + \epsilon\rho s\vartheta_2\dot{\theta}^2(t) \\ &- \kappa\epsilon EI\int_0^s \alpha'^2 dp - (\frac{\epsilon\rho}{2} - \frac{\epsilon\rho s}{\vartheta_2})\int_0^s \dot{x}^2 dp \\ &- (\frac{\epsilon I_\rho}{2} - \kappa\epsilon I_\rho)\int_0^s \dot{\alpha}^2 dp + \epsilon K s^2\vartheta_3\int_0^s \alpha'^2 dp \\ &+ (\frac{\epsilon Ks}{\vartheta_3} + \frac{\epsilon Ks}{2})[\gamma'(s,t) - \alpha(s,t)]^2 + \frac{\epsilon I_\rho s}{2}\dot{\alpha}^2(s,t) \\ &+ \epsilon K|\kappa - 1|s^2\vartheta_4\int_0^s \alpha'^2 dp + \kappa\epsilon EIs\vartheta_5\int_0^s \alpha'^2 dp \\ &+ \frac{\epsilon K|\kappa - 1|}{\vartheta_4}\int_0^s (\gamma' - \alpha)^2 dp + \frac{\kappa\epsilon EI}{\vartheta_5}\alpha'^2(s,t) \\ &- \frac{\epsilon K}{2}\int_0^s (\gamma' - \alpha)^2 dp + \frac{\epsilon EIs}{2}\alpha'^2(s,t),\end{aligned} \tag{50}$$

where $\vartheta_2 \sim \vartheta_5 > 0$.

Invoking (34) and (35), $\dot{G}_o(t)$ is calculated as

$$\begin{aligned}\dot{G}_o(t) =& -\varpi_1\varsigma_1\omega f_1\tilde{q}_1 - \varsigma_1\phi_1\tilde{q}_1(q_1 + \tilde{q}_1) - \varpi_2\varsigma_2\omega f_2\tilde{q}_2 \\ &- \varsigma_1\phi_2\tilde{q}_2(\tilde{q}_2 + q_2) - \varpi_3\varsigma_3\omega f_3\tilde{q}_3 - \varsigma_1\phi_3\tilde{q}_3(\tilde{q}_3 + q_3) \\ &+ \tilde{Q}_{1m}\varpi_1\tanh(\varpi_1) - \varphi_1\tilde{Q}_{1m}(\tilde{Q}_{1m} + Q_{1m}) \\ &+ \tilde{Q}_{2m}\varpi_2\tanh(\varpi_2) - \varphi_2\tilde{Q}_{2m}(\tilde{Q}_{2m} + Q_{2m}) \\ &+ \tilde{Q}_{3m}\varpi_3\tanh(\varpi_3) - \varphi_3\tilde{Q}_{3m}(\tilde{Q}_{3m} + Q_{3m}).\end{aligned} \tag{51}$$

Invoking (48)–(51) and using Lemmas 1 and 2 result in

$$\begin{aligned}\dot{G}(t) \leq& -(k - \frac{K}{2})\varpi_1^2(t) - (k_1 - \frac{EI}{2})\varpi_2^2(t) + \frac{\varphi_1}{2}Q_{1m}^2 \\ &- k_2\varpi_3^2(t) - \psi_1\dot{x}^2(s,t) - \psi_3\dot{\alpha}^2(s,t) + \frac{\varphi_2}{2}Q_{2m}^2 \\ &- \psi_2[\alpha(s,t) - \gamma'(s,t)]^2 - \psi_4\alpha'^2(s,t) + \frac{\varphi_3}{2}Q_{3m}^2 \\ &- \psi_5\int_0^s \dot{x}^2 dp - (k_4 - \epsilon\rho s\vartheta_2)\dot{\theta}^2(t) + \frac{\varsigma_1\phi_1}{2}q_1^2 \\ &- \psi_6\int_0^s \dot{\alpha}^2 dp - \psi_7\int_0^s \alpha'^2 dp + \frac{\varsigma_2\phi_2}{2}q_2^2 + \frac{\varsigma_3\phi_3}{2}q_3^2 \\ &- \psi_8\int_0^s (\alpha - \gamma')^2 dp - (k_3 - K\vartheta_1)e^2(t) - \frac{\varsigma_1\phi_1}{2}\tilde{q}_1^2 \\ &+ 0.2785(Q_{1m} + Q_{2m} + Q_{3m}) - \frac{\varsigma_2\phi_2}{2}\tilde{q}_2^2 \\ &- \frac{\varsigma_3\phi_3}{2}\tilde{q}_3^2 - \frac{\varphi_1}{2}\tilde{Q}_{1m}^2 - \frac{\varphi_2}{2}\tilde{Q}_{2m}^2 - \frac{\varphi_3}{2}\tilde{Q}_{3m}^2,\end{aligned} \tag{52}$$

where $\vartheta_1 > 0$ and the intermediate parameters are selected such that

$$k - \frac{K}{2} > 0, k_1 - \frac{EI}{2} > 0, k_3 - K\vartheta_1 > 0, \tag{53}$$

$$\psi_1 = \frac{K}{2} - \frac{\epsilon\rho s}{2} \geq 0, \psi_2 = \frac{K}{2} - \frac{\epsilon Ks}{\vartheta_3} - \frac{\epsilon Ks}{2} \geq 0, \tag{54}$$

$$\psi_3 = \frac{EI}{2} - \frac{\epsilon I_\rho s}{2} \geq 0, \psi_4 = \frac{EI}{2} - \frac{\epsilon EIs}{2} - \frac{\kappa\epsilon EI}{\vartheta_5} \geq 0, \tag{55}$$

$$\psi_5 = \frac{\epsilon\rho}{2} - \frac{\epsilon\rho s}{\vartheta_2} > 0, \psi_6 = \frac{\epsilon I_\rho}{2} - \kappa\epsilon I_\rho > 0, \tag{56}$$

$$\begin{aligned}\psi_7 =& \frac{\epsilon EI}{2} - \epsilon Ks^2\vartheta_3 - \epsilon K|1 - \kappa|s^2\vartheta_4 \\ &+ \kappa\epsilon EI - \kappa\epsilon EIs\vartheta_5 > 0,\end{aligned} \tag{57}$$

$$\psi_8 = \frac{\epsilon K}{2} - \frac{\epsilon K|1 - \kappa|}{\vartheta_4} - \frac{K}{\vartheta_1} > 0, k_4 - \epsilon\rho s\vartheta_2 \geq 0, \tag{58}$$

$$\begin{aligned}\sigma =& 0.2785(Q_{1m} + Q_{2m} + Q_{3m}) + \frac{\varphi_1}{2}Q_{1m}^2 + \frac{\varphi_2}{2}Q_{2m}^2 \\ &+ \frac{\varphi_3}{2}Q_{3m}^2 + \frac{\varsigma_1\phi_1}{2}q_1^2 + \frac{\varsigma_2\phi_2}{2}q_2^2 + \frac{\varsigma_3\phi_3}{2}q_3^2 < +\infty.\end{aligned} \tag{59}$$

In addition, invoking Lemma 3 and (52)–(59), we derive

$$\dot{G}(t) \leq -\delta_3[G_m(t) + G_n(t) + G_o(t)] \leq -\delta G(t) + \sigma, \tag{60}$$

where $\delta_3 = \min(\frac{2\psi_5}{\rho}, \frac{2\psi_6}{I_\rho}, \frac{2\psi_7}{EI}, \frac{2\psi_8}{K}, \frac{2k-K}{M}, \frac{2k_1-EI}{J}, \frac{2k_2}{I_h}, \frac{2k_3-2K\vartheta_1}{k_3+k_4}, \phi_1, \phi_2, \phi_3, \varphi_1, \varphi_2, \varphi_3)$ and $\delta = \delta_3/\delta_2$. ■

3.2. Stability analysis

Theorem 1. *For the Timoshenko arm system subject to actuator failures and backlash-like hysteresis described by (1)–(6), (7), and (9), with the action of boundary adaptive FTCs (30) and updating laws (34)–(35) proposed in this paper, provided that the constraints specified in (53)–(59) hold and initial conditions are bounded, we draw conclusions that the boundary-controlled system is uniformly bounded.*

Proof. We multiply (46) by $e^{\delta t}$ and then calculate the integration to obtain the following

$$\dot{G}(t)e^{\delta t} \leq -\delta e^{\delta t}G(t) + \sigma e^{\delta t}, \tag{61}$$

$$G(t) \leq G(0)e^{-\delta t} + \frac{\sigma}{\delta}(1 - e^{-\delta t}) \leq G(0)e^{-\delta t} + \frac{\sigma}{\delta}. \tag{62}$$

The use of (41), (37), and Lemma 1, we deduce

$$\begin{aligned}&\frac{K}{4s}\gamma^2(p,t) \leq \frac{K}{4}\int_0^s \gamma'^2(p,t)dp \\ &\leq \frac{K}{2}\int_0^s [\gamma'(p,t) - \alpha(p,t)]^2 dp + \frac{7Ks^2}{2}\int_0^s \alpha'^2(p,t)dp \\ &\leq \frac{7Ks^2}{EI}G_m(t) \leq \frac{7Ks^2}{EI\delta_1}G(t) \leq \frac{7Ks^2}{EI\delta_1}\left[G(0)e^{-\delta t} + \frac{\sigma}{\delta}\right].\end{aligned} \tag{63}$$

(62) and (63) further leads to

$$|\gamma(p,t)| \leq \sqrt{\frac{28s^3}{EI\delta_1}\left[G(0)e^{-\delta t} + \frac{\sigma}{\delta}\right]}, \forall p \in [0, s]. \tag{64}$$

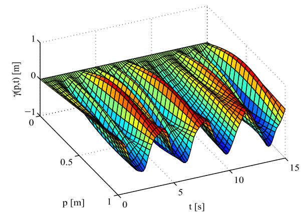

(a) Deflection of the flexible link

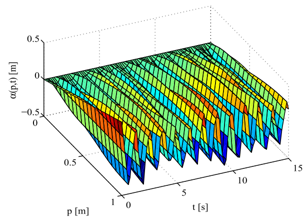

(b) Rotation of the flexible link

Fig. 4. Without control.

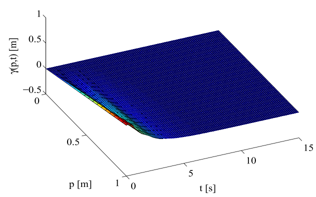

(a) Deflection of the flexible link

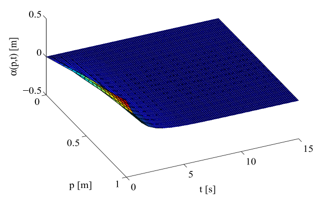

(b) Rotation of the flexible link

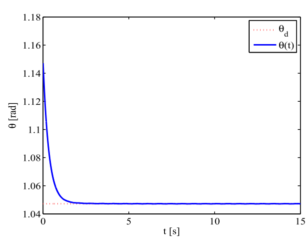

(c) Angle position of the flexible link

Fig. 5. With the proposed control (30).

Similarly, the following can be finally derived

$$|\alpha(p,t)| \le \sqrt{\frac{2s}{EI\delta_1}\left[G(0)e^{-\delta t} + \frac{\sigma}{\delta}\right]}, \forall p \in [0, s] \tag{65}$$

$$|e(t)| \le \sqrt{\frac{2}{(k_3+k_4)\delta_1}\left[G(0)e^{-\delta t} + \frac{\sigma}{\delta}\right]}. \tag{66}$$

4. Simulations

We carried out numerical simulations adopting finite difference approximation method to demonstrate the efficacy and validity of the suggested controllers in this study. The system parameters used for simulations were shown as follows: $EI = 10$ Nm^2, $s = 1.0$ m, $I_\rho = 1.0$ kgm, $J = 0.1$ kgm^2, $M = 2.0$ kg, $\rho = 1.0$ kg/m, $K = 2.0$ N, $I_h = 1.0$ kgm^2, and $\theta_d = \pi/3$ rad. The system initial conditions were appropriately described as $\gamma(p,0) = \alpha(p,0) = \frac{p}{2s}$, $\dot{\gamma}(p,0) = \dot{\alpha}(p,0) = 0$, and $\theta(0) = \pi/3 + 0.1$ rad.

The disturbances imposed on the system are provided as $d_1(t) = d_2(t) = (\sin(10\pi t) + \cos(3\pi t))/4$, $d_3(t) = \cos(3\pi t)$.

Fig. 4 displays the spatiotemporal response of the considered arm system in the free vibration, namely, $\tau_1(t) = \tau_2(t) = \tau_3(t) = 0$. When the presented adaptive FTC schemes are imposed on the studied system with the setting of design parameters as: $k = 30$, $k_1 = 55$, $k_2 = 150$, $k_3 = 300$, $k_4 = 1$, $\phi_i = \varphi_i = 0.001$, $i = 1, 2, 3$, $\omega = 1.5$, $A_{r1} = 0.5$, $A_{l1} = A_{l3} = -0.3$, $A_{r2} = 0.1$, $A_{l2} = -0.1$, $A_{r3} = 0.3$, and actuator failures occur at 1 second with fault parameters as $\varsigma_1 = 0.2$, $\varsigma_2 = 0.5$ and $\varsigma_3 = 0.3$, Fig. 5 (a) and (b) depict the 3D representation of the arm system. Fig. 5(c) shows the time history of the angle position. The responses of the presented control force and torques are portrayed in Fig. 6. The black solid line, the red line and the blue line indicate the actuator output, ideal control input and the designed control law, respectively. From the black and blue lines in the each subfigure, we can see that the actuators τ_1, τ_2 and τ_3 respectively lose 80%, 50%, 70% of their effectiveness at 1 s.

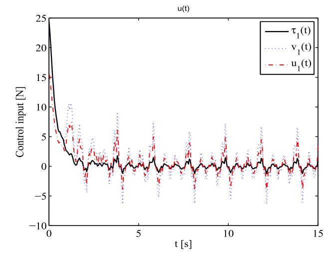

(a) Input (7), (9) and u_1

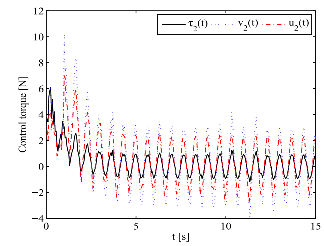

(b) Input (7), (9) and u_2

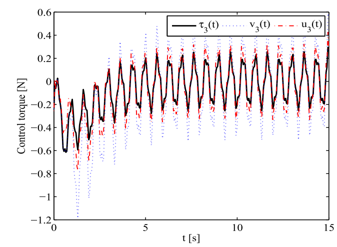

(c) Input (7), (9) and u_3

Fig. 6. Control input in (30). (For interpretation of the references to color in this figure legend, the reader is referred to the web version of this article.)

To further validate the control performance, we also provide the comparison with the existing approach proposed in He et al. (2018) formulated as

$$\begin{aligned}\tau_1(t) =& -k\varpi_1(t) - K[\alpha(s,t) - \gamma'(s,t)] \\ &+ M[\dot{\alpha}(s,t) - \dot{\gamma}'(s,t)] - \mathrm{sgn}(\varpi_1(t))\varrho_1,\end{aligned} \tag{67}$$

$$\begin{aligned}\tau_2(t) =& -k_1\varpi_2(t) + EI\alpha'(s,t) - J\dot{\alpha}'(s,t) \\ &- \mathrm{sgn}(\varpi_2(t))\varrho_2,\end{aligned} \tag{68}$$

$$\begin{aligned}\tau_3(t) =& -k_2\varpi_3(t) - k_3 e(t) - I_h\dot{\theta}(t) \\ &- k_4\dot{\theta}(t) - \mathrm{sgn}(\varpi_3(t))\varrho_3,\end{aligned} \tag{69}$$

where $k, k_1, k_2, k_3, k_4 > 0$. When the design parameters are selected as $k = 30$, $k_1 = 55$, $k_2 = 150$, $k_3 = 300$, and $k_4 = 1$, the responses of the arm system are depicted in Figs. 7–8.

The simulation results in Fig. 5 indicate that the suggested adaptive FTC can effectively restrain the arm's vibration and shear deformation and ensure the angle control despite the existence of actuator failures, hysteresis nonlinearity, and exogenous disturbances, which acquires a better control performance than the existing control in (67)–(69); and the hysteresis nonlinearity is clearly reflected in the control inputs. In a word, we arrive at a conclusion that the established control strategy can achieve the oscillation and angle control as well as handle the hybrid effects of actuator failures and hysteresis nonlinearity in the Timoshenko arm system with an excellent performance.

5. Conclusion

The boundary stabilization of flexible Timoshenko arm systems subject to actuator failures, hysteresis nonlinearity, and

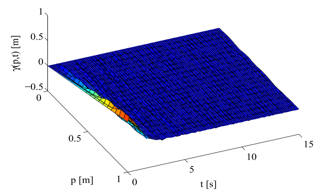

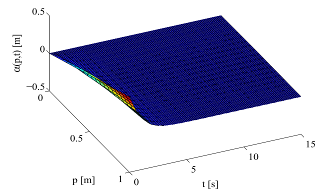

(a) Deflection of the flexible link (b) Rotation of the flexible link

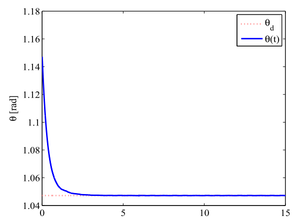

(c) Angle position of the flexible link

Fig. 7. With the existing control (67)–(69).

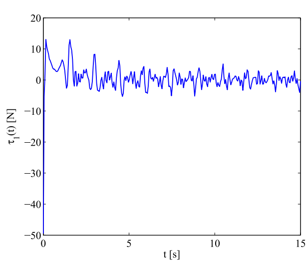

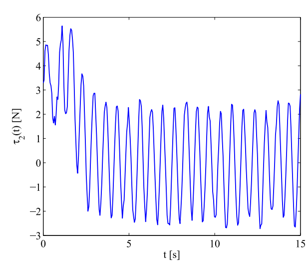

(a) Input (67) (b) Input (68)

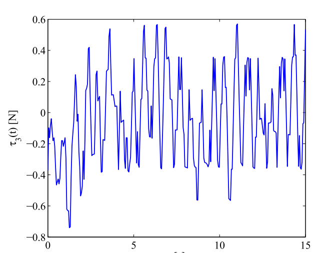

(c) Input (69)

Fig. 8. Control inputs.

exogenous disturbances has been addressed in this study. The new adaptive fault-tolerant control with unknown upper-bound dynamically updated online has been established for stabilizing vibration, achieving angle positioning, and eliminating actuator failures, backlash-like hysteresis and uncertainties of composite disturbances. The direct Lyapunov approach has been exploited to demonstrate the stability in the controlled system. In the end, simulation studies based on finite difference approximation approach have been employed to illustrate the control performance of the derived algorithm. Future interests lie in the experimental validation for Timoshenko arm systems.

Acknowledgments

This work was supported in part by National Natural Science Foundation of China under Grants 62073030, 61803109 and U20A20225, in part by the Scientific Research Projects of Guangzhou Education Bureau, China under Grant 202032793; in part by the Science and Technology Planning Project of Guangzhou City under Grant 202102010398; in part by the Science and Technology Planning Project of Guangdong Province, China under Grant 2020B0101050001, in part by a project from City University of Hong Kong under Grant 7005092, and in part by the National Research Foundation (NRF) of Korea under the auspices of the Ministry of Science and ICT, Korea under Grant NRF-2020R1A2B5B03096000.

References

Bandopadhya, D., Bhattacharya, B., & Dutta, A. (2007). An active vibration control strategy for a flexible link using distributed ionic polymer metal composites. *Smart Materials and Structures*, *16*(3), 617–625.

Boem, F., Riverso, S., Ferrari-Trecate, G., & Parisini, T. (2019). Plug-and-play fault detection and isolation for large-scale nonlinear systems with stochastic uncertainties. *IEEE Transactions on Automatic Control*, *64*(1), 4–19.

Canbolat, H., Dawson, D., Rahn, C., & Nagarkatti, S. (1998). Adaptive boundary control of out-of-plane cable vibration. *Journal of Applied Mmechanics*, *65*(4), 963–969.

Cao, F., & Liu, J. (2019). Partial differential equation modeling and vibration control for a nonlinear 3D rigid-flexible manipulator system with actuator faults. *International Journal of Robust and Nonlinear Control*, *29*(11), 3793–3807.

Dong, M., Tao, G., Wen, L., & Jiang, B. (2019). Adaptive sensor fault detection for rail vehicle suspension systems. *IEEE Transactions on Vehicular Technology*, *68*(8), 7552–7565.

Endo, T., Sasaki, M., Matsuno, F., & Jia, Y. (2017). Contact-force control of a flexible timoshenko arm in rigid/soft environment. *IEEE Transactions on Automatic Control*, *62*(2), 1004–1009.

Giri, F., Radouane, A., Brouri, A., & Chaoui, F. Z. (2014). Combined frequency-prediction error identification approach for Wiener systems with backlash and backlash-inverse operators. *Automatica*, *50*, 768–783.

Giri, F., Rochdi, Y., Radouane, A., Brouri, A., & Chaoui, F. Z. (2013). Frequency identification of nonparametric Wiener systems containing backlash nonlinearities. *Automatica*, *49*, 124–137.

Goubej, M., Vyhlídal, T., & Schlegel, M. (2020). Frequency weighted H2 optimization of multi-mode input shaper. *Automatica*, *121*, Article 109202.

Guo, K., Pan, Y., Zheng, D., & Yu, H. (2020). Composite learning control of robotic systems: A least squares modulated approach. *Automatica*, *111*, Article 108612.

He, W., Gao, H., Zhou, C., Yang, C., & Li, Z. (2020). Reinforcement learning control of a flexible manipulator: An experimental investigation. *IEEE Transactions on Systems, Man, and Cybernetics: Systems*, http://dx.doi.org/10.1109/TSMC.2020.2975232, (in press).

He, Xiuyu, He, Wei, Qin, Hui, & Sun, Changyin (2018). Boundary vibration control for a flexible timoshenko robotic manipulator. *IET Control Theory & Applications*, *12*(7), 875–882.

He, X., He, W., & Sun, C. (2017). Robust adaptive vibration control for an uncertain flexible stimoshenko robotic manipulator with input and output constraints. *International Journal of Systems Science*, *48*(13), 2860–2870.

Ibrir, S., & Su, C.-Y. (2017). Adaptive stabilization of a class of feedforward nonlinear systems subject to unknown backlash-hysteresis inputs. *IEEE Transactions on Control Systems Technology*, *25*(4), 1180–1192.

Khalili, M., Zhang, X., Cao, Y., Polycarpou, M., & Parisini, T. (2020). Distributed fault-tolerant control of multiagent systems: An adaptive learning approach. *IEEE Transactions on Neural Networks and Learning Systems*, *31*(2), 420–432.

Khalili, M., Zhang, X., Polycarpou, M., Parisini, T., & Cao, Y. (2018). Distributed adaptive fault-tolerant control of uncertain multi-agent systems. *Automatica*, *87*, 142–151.

Koga, S., & Krstic, M. (2020). Arctic sea ice state estimation from thermodynamic PDE model. *Automatica*, *112*, Article 108713.

Liu, Z., Han, Z., Zhao, Z., & He, W. (2020). Modeling and adaptive control for a spatial flexible spacecraft with unknown actuator failures. *Science China Information Sciences*, *64*(5), Article 152208.

Morgul, O. (1991). Boundary control of a Timoshenko beam attached to a rigid body: Planar motion. *International Journal of Control*, *54*(4), 763–791.

Polycarpou, M. M., & Ioannou, P. A. (1996). A robust adaptive nonlinear control design. *Automatica*, *32*(3), 423–427.

Shi, D.-H., Feng, D.-X., & Yan, Q.-X. (2001). Feedback stabilization of rotating timoshenko beam with adaptive gain. *International Journal of Control*, *74*(3), 239–251.

Su, C.-Y., Stepanenko, Y., Svoboda, J., & Leung, T. P. (2000). Robust adaptive control of a class of nonlinear systems with unknown backlash-like hysteresis. *IEEE Transactions on Automatic Control*, *45*(12), 2427–2432.

Tao, G., & Kokotovic, P. V. (1996). *Adaptive control of systems with actuator and sensor nonlinearities*. New York, NY, USA: Wiley.

Wang, Ji, & Krstic, Miroslav (2020). Delay-compensated control of sandwiched ODE–PDE–ODE hyperbolic systems for oil drilling and disaster relief. *Automatica*, *120*, Article 109131.

Wang, H., Liu, P. X., Zhao, X. D., & Liu, X. (2020). Adaptive fuzzy finite-time control of nonlinear systems with actuator faults. *IEEE Transactions on Cybernetics*, *50*(5), 1786–1797.

Yang, Xu, Gao, Jingjing, Li, Linlin, Luo, Hao, Ding, Steven X., & Peng, Kaixiang (2020). Data-driven design of fault-tolerant control systems based on recursive stable image representation. *Automatica*, *122*, Article 109246.

Yu, Z. X., Li, S. G., Yu, Z. S., & Li, F. F. (2018). Adaptive neural output feedback control for nonstrict-feedback stochastic nonlinear systems with unknown backlash-like hysteresis and unknown control directions. *IEEE Transactions on Neural Networks and Learning Systems*, *29*(4), 1147–1160.

Zhang, H., Liu, Y., Dai, J., & Wang, Y. (2020). Command filter based adaptive fuzzy finite-time control for a class of uncertain nonlinear systems with hysteresis. *IEEE Transactions on Fuzzy Systems*, http://dx.doi.org/10.1109/TFUZZ.2020.3003499, (in press).

Zhao, Z. J., & Ahn, C. K. (2020). Boundary antisaturation vibration control design for a flexible timoshenko robotic manipulator. *International Journal of Robust and Nonlinear Control*, *30*(3), 1098–1114.

Zhao, Z. J., He, X. Y., & Ahn, C. K. (2019). Boundary disturbance observer-based control of a vibrating single-link flexible manipulator. *IEEE Transactions on Systems, Man, and Cybernetics: Systems*, *51*(4), 2382–2390.

Zhou, J., Zhang, C., & Wen, C. (2007). Robust adaptive output control of uncertain nonlinear plants with unknown backlash nonlinearity. *IEEE Transactions on Automatic Control*, *52*(3), 503–509.

Zhijia Zhao received his B.Eng. degree in automatic control from North China University of Water Resources and Electric Power, Zhengzhou, China, in 2010, and his M.Eng. and Ph.D. degrees in automatic control from South China University of Technology, Guangzhou, China, in 2013 and 2017. He is currently an Associate Professor in the School of Mechanical and Electrical Engineering, Guangzhou University. His research interests include adaptive and learning control, flexible mechanical systems, ocean cybernetics, and robotics.

Zhijie Liu received B.Eng. degree from China University of Mining and Technology Beijing, Beijing, China in 2014, and the Ph.D. degree from Beihang University, Beijing, China, in 2019. In 2017, he was a Research Assistant with the Department of Electrical Engineering, University of Notre Dame, for twelve months. He is currently an Associate Professor with the School of Automation and Electrical Engineering, University of Science and Technology Beijing, Beijing, China. He is a recipient of the IEEE SMC Beijing Capital Region Chapter Young Author Prize Award in 2019. He is a member of IEEE SMC Technical Committee on Autonomous Bionic Robotic Aircraft. His research interests include adaptive control, modeling and vibration control for flexible structures, and distributed parameter systems.

Wei He is currently working as a Full Professor in School of Automation and Electrical Engineering, University of Science and Technology Beijing, Beijing, China. He has co-authored 3 books published in Springer and published over 100 international journal and conference papers. He is serving as an Associate Editor of IEEE Transactions on Robotics, IEEE Transactions on Neural Networks and Learning Systems, IEEE Transactions on Control Systems Technology, SCIENCE CHINA Information Sciences, IEEE/CAA Journal of Automatica Sinica, and an Editor of Journal of Intelligent & Robotic Systems. He is the member of IEEE CSS Conference Editorial Board (CEB). His current research interests include robotics, distributed parameter systems and intelligent control systems.

Keum-Shik Hong received his B.S. degree in Mechanical Design and Production Engineering from Seoul National University in 1979, his M.S. degree in Mechanical Engineering from Columbia University, New York, in 1987, and both an M.S. degree in Applied Mathematics and a Ph.D. in Mechanical Engineering from the University of Illinois at Urbana-Champaign in 1991. He joined the School of Mechanical Engineering at Pusan National University (PNU) in 1993. His Integrated Dynamics and Control Engineering Laboratory was designated a National Research Laboratory by the Ministry of Science and Technology of Korea in 2003. In 2009, under the auspices of the World Class University Program of the Ministry of Education, Science and Technology of Korea, he established the Department of Cogno-Mechatronics Engineering, PNU. Dr. Hong served as Associate Editor of Automatica (2000–2006), as Editor-in-Chief of the Journal of Mechanical Science and Technology (2008–2011), and is serving as Editor-in-Chief of the International Journal of Control, Automation, and Systems. He was a past President of the Institute of Control, Robotics and Systems (ICROS), Korea, and is President of the Asian Control Association. He was the Organizing Chair of the ICROS-SICE International Joint Conference 2009, Fukuoka, Japan. He is an IEEE Fellow, a Fellow of the Korean Academy of Science and Technology, an ICROS Fellow, a Member of the National Academy of Engineering of Korea, and many other societies. He has received many awards including the Best Paper Award from the KFSTS of Korea (1999), the F. Harashima Mechatronics Award (2003), the Automatica Certificate of Outstanding Service (2006), the Presidential Award of Korea (2007), the Premier Professor Award (2011), etc. Dr. Hong's current research interests include brain–computer interface, nonlinear systems theory, adaptive control, distributed parameter systems, autonomous vehicles, and innovative control applications in brain engineering.

Han-Xiong Li received his B.E. degree in aerospace engineering from the National University of Defense Technology, China in 1982, M.E. degree in electrical engineering from Delft University of Technology, The Netherlands in 1991, and Ph.D. degree in electrical engineering from the University of Auckland, New Zealand in 1997. He is a Professor in the Department of SEEM, City University of Hong Kong. He has broad experience in both academia and industry. He has authored 2 books and about 20 patents, and published more than 200 SCI journal papers with h-index 46 (web of science). His current research interests include process modeling and control, system intelligence, distributed parameter systems, and battery management system. Dr. Li serves as Associate Editor for IEEE Transactions on SMC: Systems, and was Associate Editor for IEEE Transactions on Cybernetics (2002–2016) and IEEE Transactions on Industrial Electronics (2009–2015). He was awarded the Distinguished Young Scholar (overseas) by the China National Science Foundation in 2004, a Chang Jiang professorship by the Ministry of Education, China in 2006, and a national professorship in China Thousand Talents Program in 2010. He serves as a distinguished expert for Hunan Government and China Federation of Returned Overseas Chinese. He is a Fellow of the IEEE.